Proceedings of the 18th Annual North American Waste-to-Energy Conference
NAWTEC18
May 11-13, 2010, Orlando, Florida, USA

NAWTEC18-3554

HIGH TEMPERATURE CORROSION IN A 24 MW WASTE-TO-ENERGY PLANT

Wenchao Ma
Tianjin University, School of Environmental Science and Technology / State Key Laboratory of Engines
Tianjin, China

Vera Susanne Rotter
Berlin University of Technology, Institute of Environmental Technology
Berlin, Germany

Dezhou Shao
Tianjin TEDA environmental protection company, LTD,
Tianjin, China

Guanyi Chen
Tianjin University, School of Environmental Science and Technology / State Key Laboratory of Engines
Tianjin, China

ABSTRACT

Waste-to-energy (WTE) plants are utilized for the production of heat and electricity from municipal solid waste (MSW) and refuse derived fuel (RDF). Due to high chlorine content (0.5wt.%~1.0wt.%) in MSW & RDF, high temperature corrosion is often observed on the superheater surfaces and correspondingly leads to a very low efficiency of 15%~25% in practical WTE plants. To obtain information on the corrosion rate and high temperature corrosion mechanism, a full scale nine-month-long term corrosion test was therefore conducted in a heat and power generating WTE plant in Tianjin, China. The grate boiler with a capacity of 400 tons/d, runs at a burning temperature between 850~900ºC, flue gas temperature between 550~650ºC, steam temperature of 400ºC, and steam pressure of 4MPa. The corrosion probes made of same metal alloy with heat exchanger were exposed on the surface of economizer, protector and superheater, respectively. The metal loss by corrosion was determined by measuring the distance from the inside of the ring to the interface between metal and oxide with a measuring microscope. The deposit characteristics as well as elemental compositions were determined using a scanning electron microscope (SEM) and energy dispersive spectrometer (EDS). The objective of this work is to evaluate: 1) plant specific corrosion rate on different superheater materials and 2) relationship among chlorine content in the feedstock, chlorine gas emission before air pollutant clean system, and deposits composition. The results showed deposits characteristics depend on the probe location, metal materials, temperature and windward/leeward. Barely chlorine exists in the deposits, except for the outer surface of the deposits at 3rd SH. The highest corrosion loss for 20G at 3rd SH was calculated to be 2mm/year, based on the assumption of linear extrapolation of corrosion rate.

Keywords: Waste-to-energy (WTE), municipal solid waste (MSW), chlorine, high temperature corrosion

1. INTRODUCTION

Municipal solid waste (MSW) and refuse derived fuel (RDF) are utilized for heat and electricity production in waste-to-energy (WTE) plants. Nowadays, around 130 million ton of MSW are incinerated worldwide in WTE plants [1], and about 380 WTE plants across EU [2]. By the end of 2005, 67 MSW incinerators run with a treatment capacity of 33 010 tons/d in China, accounting for 13% of total MSW treatment [3]. In the US alone, about 28 million tons of MSW are combusted annually in WTE facilities to produce about 2.8 GW (10^9 watts) of electricity and some steam for district heating plants [1]. Whereas, high chlorine content (~1.0wt.%) in the waste plays a dominant role in high temperature corrosion on superheater surfaces [4-5], which constitutes significant operational problems, such as loss of material, frequent shut-downs for maintenance, and high operational cost in WTE plants [6]. To minimize corrosion, it is quite often in practical to reduce the steam temperature to 400°C~420°C, which correspondingly reduces the energy efficiency to less than ~25% [7]. In comparison, the modern coal-fired plant with a chlorine content

Copyright © 2010 by ASME

of maximum levels~0.25wt.%, is able to reach the electrical efficiency of 47% (580°C and 289 bar steam pressure) [8]. Thus, there is a strong need to study the high temperature corrosion mechanism and bridge it with chlorine content in the fuel management.

Our previous study identified chlorine in MSW originating mainly from polyvinyl chloride (PVC) and sodium chloride (NaCl) [9]. Albina et al. [10] studied the effects of feed composition on boiler corrosion in WTE plants through thermodynamic calculations and concluded that an increase in chlorine content of the fuel leads to higher production of gaseous HCl, KCl, NaCl and condensed phases of NaCl, KCl, which were perceived to be the precursors of corrosion. Persson et al. [5] studied high temperature corrosion in a WTE plant by varying the feedstock with additional PVC, and compared the corrosion rates of five different alloys. Nielsen [11] performed several deposition and corrosion tests in biomass fired boilers.

To obtain information on the corrosion rate and high temperature corrosion mechanism, a full scale nine-month-long term corrosion test was therefore conducted in a power and heat generating WTE plant in Tianjin, China. Several corrosion probes made of two different alloys were set at convective pass and exposed in the boiler. The objectives of this work were to evaluate: 1) plant specific corrosion rate on different superheater materials and 2) relationship among chlorine content in the feedstock, chlorine gas emission before air pollutant clean system, and deposits composition.

2. EXPERIMENTAL

2.1 Materials

The waste comes from two downtown districts and one urban district, where the living standard of people is higher than other districts in Tianjin. Table 1 shows the waste composition in Hexi District, Tianjin each month in 2009. The food fraction in Tianjin, similar to other Chinese cities, takes the largest weight proportion (around 50wt.%), whereas in developed countries paper and cupboard making up the largest fraction. The paper and plastics fractions contribute 40wt.% to total waste, which differs from most Chinese cities. The weight proportion of these fractions in Beijing is 23.7wt.% [12], Shanghai of 27.0wt.% [12], Hangzhou of 26.8wt.% [14], and Guangzhou of 14.4wt.% [3]. The high proportion may be attributed to the high living standard of residence in that area. Moreover, recyclable fractions like metal, glass contribute less than 5wt.% to waste streams, since they are efficiently recycled by waste picker before centralized collection, due to high values.

In our previous paper [9], we identified the food residues and plastics as the main chlorine sources, containing high chlorine concentration of 0.9% and 0.5~6.3%, respectively. Due to the large food residue and plastic proportion, the chlorine content of MSW in Tianjin is severe high to 1.13% (Table 2), which may easily result into chlorine induced high temperature corrosion. Furthermore, the large proportion of food residues also leads to the high moisture content (~50%) in waste.

Table 1. Waste composition in terms of months in Hexi District, Tianjin, China, 2009 (wt.%)

Month	Organic		Inorganic		Recyclable						Others
	Food	Shell	Ash	Bricks	Metals	Glasses	Paper	Plastics	Textiles	Grass	
1	52.4	0.2	1.5	0.1	0.1	6.7	18.6	14.4	2.4	1.3	2.6
2	51.9	0.3	0.9	0.1	2.2	7.9	17.4	15.1	2.0	1.2	1.0
3	30.4	0.1	0.6	0.2	0.4	5.7	26.5	30.8	0.8	4.4	0.2
4	43.6	1.4	0.6	0.4	0.2	0.1	17.5	25.8	0.0	0.1	0.4
5	50.3	0.1	1.5	0.5	0.2	0.4	21.8	21.8	2.2	0.9	0.5
6	48.3	1.0	0.1	0.7	1.0	1.6	21.1	22.3	2.0	0.1	2.0
7	48.3	0.3	0.5	1.3	0.1	7.5	11.9	20.2	5.4	2.0	2.4
8	54.9	0.2	1.9	1.9	0.2	3.1	14.6	17.2	0.2	2.7	3.2
9	48.2	1.5	0.8	0.2	0.3	0.5	22.6	24.0	0.1	0.3	1.6
10	48.3	0.2	0.3	0.3	0.4	6.7	22.9	18.0	1.3	0.9	0.8
11	53.4	0.4	0.9	0.2	0.3	3.5	20.9	17.4	0.1	2.0	0.6
12	50.2	0.9	0.5	0.2	0.4	5.9	16.1	17.4	1.8	6.6	0.1
Average	48.4	0.5	0.8	0.5	0.5	4.1	20.2	20.4	1.6	1.9	1.3

Copyright © 2010 by ASME

Table 2. Proximate analysis and ultimate analysis of waste in Tianjin

	Proximate analysis (%)				Ultimate analysis (%)					
	Moisture	Volatile	Ash	Low heating value (kJ/kg)	C	H	O	N	S	Cl
MSW	46.7	41.4	11.9	6480	43.26	7.87	45.21	2.45	0.08	1.13

2.2 Plant introduction

Experiments were conducted at a heat and power generating WTE plant (Teda Environmental Protection. Ltd) in Tianjin, China. This plant consists of three SN grate boilers with a total design capacity of 1200 tons household MSW per day, and two 12MW steam turbine generators, commissioned in 2004~2005 (Fig.1). The Unit 1 specifications and its operational parameters are shown in Table3. During the experiments, the boiler was running stably and did not experience malfunctions.

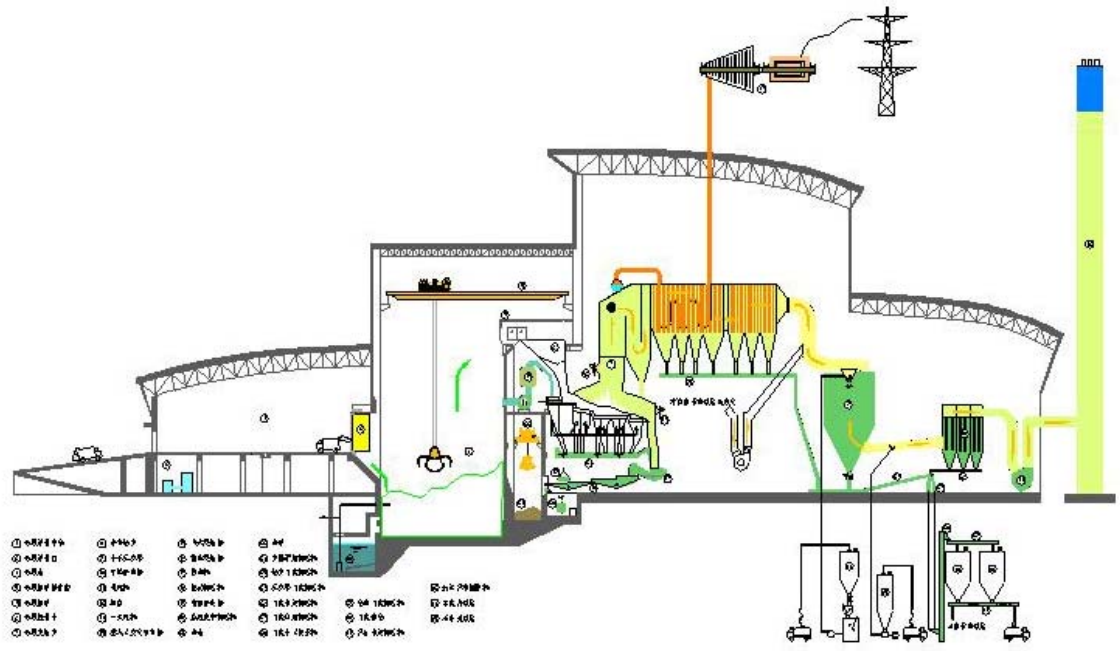

Figure 1. Schematic diagram of TEDA waste-to-energy plant in Tianjin

Table 3. Specifications and operating parameters of Unit 1 boiler

Nominal capacity	Nominal electricity production	Primary air flow	Secondary air flow	Steam temperature	Steam pressure
400tons/day	24MW	25~30 km^{3}N/h	5~7 km^{3}N/h	400℃	40bar

2.3 Probe settings

To observe the corrosion rate and chlorine induced high temperature corrosion phenomenon, a full scale nine-month-long term corrosion test was conducted using corrosion probes without cooling system at different flue gas passes. The flue gas passes through the furnace chamber, the secondary burning chamber in the second pass of boiler, the pre-protector, the tertiary superheater (3rd SH), secondary superheater (2nd SH), and primary superheater (1st SH). After primary superheater, the gas passes through the evaporator, three economizers (3rd EC, 2nd EC, 1st EC). Finally, the fly ash particles are removed in a semi-dry scrubber (Fig.2).

The materials of corrosion probes were selected in terms of the materials used for the superheater tubes (Table 4). Chemical composition of tested alloys is shown in Table 5. Several thermocouples were set near the probes to monitor the flue gas temperature.

After exposure, the corrosion probes were carefully dismounted. Afterwards, the rings were cut in six pieces and the

Copyright © 2010 by ASME

cross sections were polished and dried for further analyses. Hereby the integrity of the oxides and deposits were preserved. The metal loss by corrosion was determined by measuring the distance from the inside of the ring to the interface between metal and oxide with a measuring microscope. The alloys characteristics as well as elemental compositions were determined by analyses of the polished cross sections using a scanning electron microscope/ energy dispersive spectrometer (PHILIPS XL-30 TMP ESEM, 20kV, Holland). Meanwhile, the deposits on probes in terms of its growing direction were separated and collected to observe the chemical composition variations.

Table 4. Tube materials and probe materials in different locations

Location	Waterwall	Pre-protector	3rd SH	2nd SH	1st SH	Evaporator	3rd EC	2nd EC	1st EC
Tube material	20G		TP310H	15CrMoG		20G			
Probe material & size	-	20G (R38*7)	20G (R43*3), 15CrMoG	-	20G (R43*3)	20G(R43*3), 15CrMoG	-	-	20G (R38*7)

Table 5. Chemical composition of tested alloys, Fe is balance

	C	Mn	Si	Cr	Mo	S	P
20G	0.17~0.24	0.35~0.65	0.17~0.37	_	_	0.030	0.030
15CrMoG	0.12~0.18	0.40~0.70	0.17~0.37	0.80~1.10	0.40~0.55	0.030	0.030

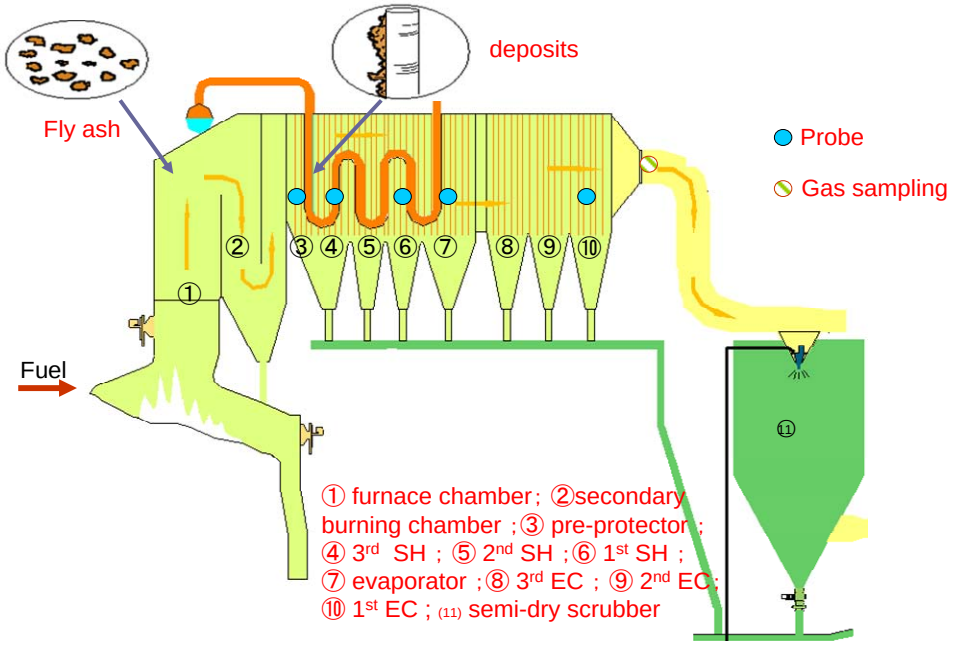

Fig. 2. Schematic diagram of boiler and convective pass

3. RESULTS & DISCUSSION

3.1 Deposits characterization on probes

Visible amount of deposits were formed on the probes, varying depth and color with locations (Table 6). The deposit on the windward side was more dense and darker than that on the leeward side. Meanwhile, the dense deposit is also more difficult to brush off. The deposit collected on 3rd SH probe was dark red, in comparison with other deposits in light gray. It had an inner uniform layer with islands of deposit on top of this. The islands probably acted as initiators for further deposition growth. Thus, more attention was paid to the deposit on 3rd SH according to its growing direction, which was categorized into outer deposit, middle deposit and inner deposit (Fig.3). The deposits used for chemical analysis were scraped from the test probe and represent an average value of the deposits on the windward and the leeward side. The deposits were rich in

Copyright © 2010 by ASME

potassium and sulfur, to a lesser content in calcium and silicon, and some sodium, magnitude, aluminum. Barely chlorine exists in the most deposits, except for the outer surface of the deposits at 3rd SH.

3.2 Corrosion on different metals

To determine the influence of different tube materials on corrosion, the probes made of 20G and 15CrMoG on 3rd SH were analyzed. The inner layer of deposit, next to the metal oxide layer, is of particular interest in regard to corrosion of the superheater tubes. The SEM analyses revealed a major difference in the appearance of the inner lay of deposit on tube materials of 20G and 15CrMoG, respectively.

3.3 Corrosion rate

Significant differences in corrosion rates were found among probes at different location. The highest average corrosion loss for 20G occurred to 3rd SH and was calculated to be 2mm/year. The calculation adopted the assumption that corrosion rate was linear, which was based on the fact that oxide layers formed during corrosion do not provide an effective protection against further corrosion attack. Linear extrapolation of corrosion rates may result in an overestimation due to the influence of the higher rate of initial corrosion. However, it can be a worst-case approximations as well as for comparing materials.

Negligible corrosion was observed on the other probes, which revealed a strong temperature dependence on corrosion with markedly increased corrosion rates at higher temperatures. Nielsen [11] point out corrosion was negligible with a rate of less than 0.01mm/1000h for metal temperature below 480℃, a tendency for increased corrosion of 0.1mm/1000h with temperature among 520~550℃, and dramatically increasing corrosion of 1mm/1000h at temperature above 600℃.

Table 6. Physical and chemical composition of deposits on oxygen free basis

Location	Depth of deposition (windward / leeward)	Color	Temperature	Elemental analyzer [wt.%]							
	mm		℃	Na	Mg	Al	Si	S	Cl	K	Ca
Pre-protector	3/1		660.7±24.8	6	1.01	1.09	2.1	17.08	0	15.84	7.17
3rd SH (mixture)	8/3	Dark red	619.6±18.7	4.51	1.01	0.82	1.10	0.97	0	11.18	7.43
3rd SH (outer)		Dark red		2.08	0.69	6.97	7.01	3.19	10.59	1.03	27.37
3rd SH (middle)		Light white		7.74	0.51	0.48	0.99	19.12	0	16.91	4.73
1st SH	10/8	Grey	397.4±7.8	0.31	2.50	1.07	5.06	17.04	0	8.65	13.35
Evaporator	5/3.5	Light white	338.1±5.4	9.18	0.65	0.77	1.38	21.18	0	17.04	8.10
1st EC	5/3	Light grey	193.4±3.5	4.58	1.03	0.69	0.86	16.71	0	13.95	7.17-
Semi-dry scrubber	-		159.8±0.3								
Stack	-		151.0±0.7								

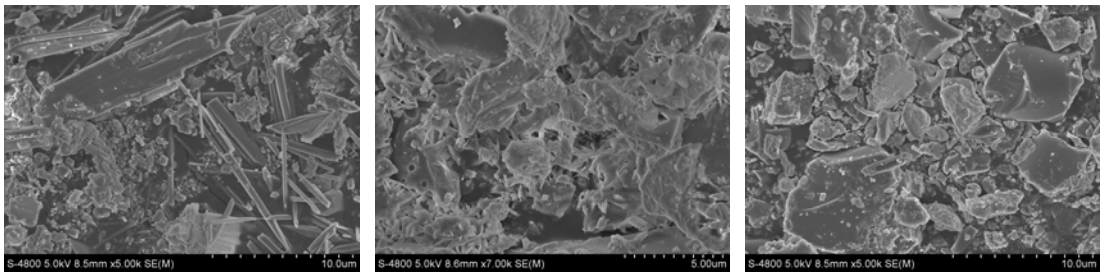

Fig.3 SEM of outer deposit (left), middle deposit (middle) and mixture deposit (right) on 3rd SH

Copyright © 2010 by ASME

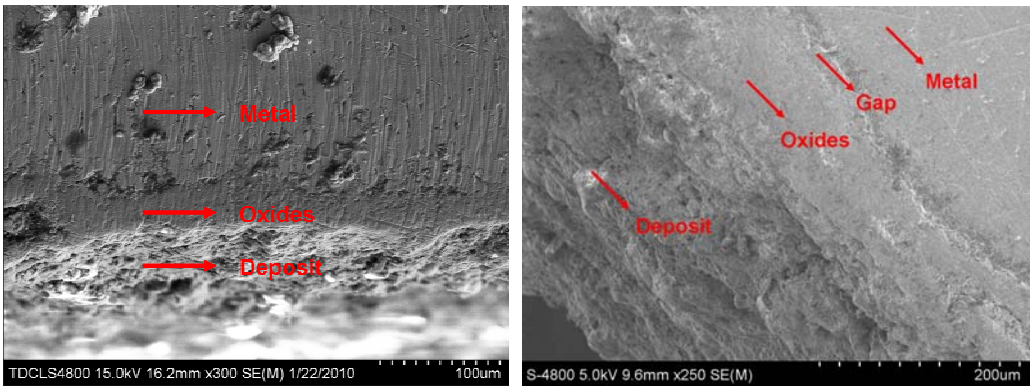

Fig 4. SEM micrograph of 15CrMoG (left) and 20G (right), at 3rd SH

4. CONCLUSION

Based on the work thus far, following conclusion can be made:

① . Deposits characteristics depend on the probe location, metal materials, temperature and windward/leeward.

② . Barely chlorine exists in the deposits, except for the outer surface of the deposits at 3rd SH.

③ . The highest corrosion loss for 20G at 3rd SH was calculated to be 2mm/year, based on the assumption of linear extrapolation of corrosion rate.

ACKNOWLEDGEMENT

This work was partly sponsored by International S&T Cooperation through the MOST (Grant No. 2006DFA62370), and China Natural Science Foundation (Grant No. 90610020).

REFERENCES

[1] D. O. Albina, Theory and experience on corrosion of waterwall and superheater tubes of waste to energy facilities, Doctoral thesis, Columbia University, USA, August 2005.

[2] http://www.cewep.com/?fCMS=af554e7670e29d2b05fefd1824a11090, Retrived on 2010.03.12

[3] Y. Zhang, Y. Chen, A. Meng, Q. Li, H. Cheng, Experimental and thermodynamic investigation on transfer of cadmium influenced by sulfur and chlorine during municipal solid waste (MSW) incineration, Journal of Hazardous Materials 153 (2008) 309–319.

[4] W. Ma, S. Rotter, Overview on the chlorine origin of MSW and Cl-originated corrosion during MSW & RDF combustion process, in: Second International Environment and Public Health Track, Shanghai, China, 2008.

[5] K. Persson, M. Brostrom, J. Carlsson, A. Nordin, R. Backman, High temperature corrosion in a 65MW waste to energy plant, Fuel processing technology 88 (2007) 1178-1182.

[6] M. Bøjer, P. Jensen, F. Frandsen, K. Johansen, O. Madsen, K. Lundtorp, Alkali/Chloride release during refuse incineration on a grate: Full-scale experimental findings, Fuel Process. Technol. 89 (5) (2008) 528-539.

[7] P. Redmakers, W. Hesseling, de W. J.van, Review on corrosion in waste incinerators, TNO report, 2003.

[8] J. Buggea, S. Kjæra, R. Blum, High-efficiency coal-fired power plants development and perspectives, Energy 31 (2006) 1437–1445.

[9] W. Ma, G. Hoffmann, M. Schirmer, G. Chen, V.S. Rotter, Chlorine characterization and thermal behavior in MSW and RDF, Journal of Hazardous Material, 2010, doi:10.1016/j.jhazmat.2010.01.108, in Press.

[10] D.O.Albina, Karsten Millrath, N.J.Themelis, Effects of feed composition on boiler corrosion in waste-to-energy plants, 12th NAWTEC, Savannah, USA, 2004.

[11] H. P. Nielsen, Deposition and high temperature corrosion in biomass fired boilers, Doctoral thesis, Technical University of Denmark, 1998, Denmark..

[12] Z. Li, L. Yang, X. Qu, Y. Sui, Municipal solid waste management in Beijing City, Waste Management 29 (2009) 2596 – 2599.

[13] L. Su, Potential of Waste-to-Energy Technologies and the use of Refuse Derived Fuel (RDF) in China - Impact on Reduction of GHG emission, Master thesis of TU Berlin, Germany, July 2009.

[14] Y. Zhuang, S.W Wu, Y.L Wang, W.X Wu, Y.X Chen, Source separation of household waste: A case study in China, Waste Management 28 (2008) 2022 – 2030.

Copyright © 2010 by ASME